

SNV-FEAST: microbial source tracking with single nucleotide variants

Leah Briscoe^{1*}, Eran Halperin^{2,3,4,5,6}, Nandita R. Garud^{3,7*}

1. Bioinformatics Interdepartmental Program, University of California Los Angeles, Los Angeles, Los Angeles, CA, United States of America
2. Department of Computer Science, University of California Los Angeles, Los Angeles, CA, United States of America
3. Department of Human Genetics, David Geffen School of Medicine, University of California Los Angeles, Los Angeles, CA, United States of America
4. Department of Computational Medicine, David Geffen School of Medicine, University of California Los Angeles, Los Angeles, CA, United States of America
5. Department of Anesthesiology and Perioperative Medicine, David Geffen School of Medicine, University of California Los Angeles, Los Angeles, CA, United States of America
6. Institute of Precision Health, University of California Los Angeles, CA, United States of America
7. Department of Ecology and Evolutionary Biology, University of California Los Angeles, CA, United States of America

*Correspondence to leahpbriscoe@gmail.com and ngarud@ucla.edu

22 **ABSTRACT**

23 Elucidating the sources of a microbiome can provide insight into the ecological dynamics
24 responsible for the formation of these communities. “Source tracking” approaches to date
25 leverage species abundance information, however, single nucleotide variants (SNVs) may be
26 more informative because of their high specificity to certain sources. To overcome the
27 computational burden of utilizing all SNVs for a given sample, we introduce a novel method to
28 identify signature SNVs for source tracking. We show that signature SNVs used as input into a
29 previously designed source tracking algorithm, FEAST, can more accurately estimate
30 contributions than species and provide novel insights, demonstrated in three case studies.

31

32 **Keywords:** Source tracking, microbiome, single nucleotide variants, transmission, strains

33

34 **BACKGROUND**

35 Understanding the sources that could contribute to the formation of a given microbiome
36 is of great interest in elucidating the ecological processes that give rise to these complex
37 communities and the impact of these communities on human and environmental health. For
38 example, a hospital environment may introduce antibiotic resistance genes to an infant gut
39 microbiome, and local selective pressures may result in vastly different microbial compositions
40 in different parts of the ocean. Approaches for determining the proportion of a microbiome of
41 interest (the “sink”) that is attributed to different microbiomes (the “sources”) is known as
42 “source tracking” (Knights et al., 2011; Shenhav et al., 2019). Source tracking is useful for
43 forensics, categorization of samples, detecting contamination, and tracing transmissions between
44 different hosts or environments. While source tracking was developed as a way to quantitatively
45 characterize a sample based on a set of samples with known origin, in most studies, the true
46 source of samples may never be collected. In these cases, source tracking approaches are useful
47 in identifying similarities between microbiome samples even if they cannot be used to
48 definitively identify the true source of origin.

49 Current approaches for source tracking include the Bayesian approach, SourceTracker
50 (Knights et al., 2011) and more recently the expectation-maximization approach, FEAST
51 (Shenhav et al., 2019). These source tracking methods use species abundance profiles of the
52 sample of interest (the sink) and of potential sources and compute percentages of sinks that are
53 attributable to each potential source. However, species abundance profiles miss important sub-
54 species single nucleotide variants (SNVs), which may provide higher resolution information than
55 species about transmission patterns. For example, (Nayfach et al., 2016) found that the sharing of
56 microbiome SNVs private to mothers and their infants decreases over the first year of the
57 infant’s life while species sharing increases. This suggests that while the infant microbiome
58 increasingly resembles the adult microbiome ecologically, sources other than the mother also
59 colonize the infant. Thus, species-level resolution may obscure true sources of microbes while
60 SNVs can reveal actual transmissions to the infant.

61 While tracking strain transmissions with SNVs has been highly successful in a number of
62 studies (Asnicar et al., 2017a; Ferretti et al., 2018; Korpela et al., 2018; Li et al., 2016; Nayfach
63 et al., 2016; Olm et al., 2021; Schmidt et al., 2019) current approaches to strain tracking are
64 limited. These methods provide binary information by inferring whether or not a strain

65 transmission has occurred per species but they do not shed light on the relative proportions of
66 microbiomes that are similar. A specific example of this is inStrain (Olm et al., 2021) which
67 computes a pairwise population-level average nucleotide identity (popANI) between two
68 samples. If an infant harbors several strains derived from the mother at low frequency, these
69 shared strains will have high popANI values, but they will represent a relatively small proportion
70 of the infant's microbiome. By contrast, source tracking allows us to simultaneously infer the
71 putative proportions for multiple sources contributing to a given sink, integrated over all
72 community members in the sink. As shown in **Figure 1**, one may be able to estimate that an
73 infant microbiome is explained 25% by the mother, 10% by the dog, and 30% by unknown
74 sources (Knights et al., 2011; Shenhav et al., 2019). In other words, source tracking with SNVs
75 leverages not only the genetic variants within species, but also the relative abundances of the
76 species that carry the SNVs.

77 Here, we evaluate whether source contributions estimated with SNVs are more accurate
78 than with only species when provided as inputs to FEAST (Shenhav et al., 2019) (hereafter
79 referred to as SNV-FEAST and species-FEAST, respectively). FEAST (Shenhav et al., 2019) is
80 faster and more accurate than previous source tracking tools (Knights et al., 2011), and therefore,
81 is ideal for adaptation to SNV source tracking since it can accept larger numbers of features and
82 input sources. Despite this improved computational efficiency, the potentially millions of single
83 nucleotide variants across all microbiome species in a given host still can computationally
84 overwhelm FEAST. To address this, we introduce a novel approach to determine signature SNVs
85 that can be used as input to FEAST. This both reduces memory requirements and computation
86 time in the FEAST estimation, allowing us to optimally estimate the source contribution of a
87 sink. We find that SNV-FEAST and species-FEAST yield different outcomes when applied to
88 simulated data, with SNV-FEAST frequently out-performing species-FEAST. We apply SNV-
89 FEAST to three real-world case studies, including source tracking between infants and their
90 mothers in the first year of life, between infants and the neonatal intensive care unit (NICU), and
91 between oceans around the world. We confirm the ability of SNV-FEAST by recapitulating
92 several previously published findings in our case studies, as well as discover new source tracking
93 patterns across oceans. In sum, we show that SNVs can be used to estimate potential
94 transmissions across hosts and across environments.

95

96 **RESULTS**

97

98 **SNV-FEAST algorithm**

99 Here we adapt FEAST to accept SNV abundance instead of species abundance as input.

100 A computational challenge in using SNVs instead of species as input to FEAST is that SNVs
101 contribute a significantly larger feature space. The number of different species comprising a
102 microbiome can range from a few hundred to a few thousand, while the number of possible
103 SNVs for a given species alone can be in the thousands (Schloissnig et al., 2013). This difference
104 in number of input features can result in FEAST runtimes that last several hours instead of a few
105 minutes and memory intensive storage of read counts at all sites of variation.

106 We devised a likelihood-based approach for selecting a set of informative or “signature”
107 SNVs for a given source tracking analysis, allowing us to overcome the time and memory
108 intensive challenges of utilizing SNV-level data. We identify these informative SNVs by
109 computing a signature score (**Figure 1A**) (see **Methods**) that quantifies the extent to which
110 SNVs in the sink are most likely derived from one of the potential sources. This is analogous to
111 identifying SNVs private to sources and their sinks, but more generalized to include SNVs that
112 may be found in multiple sources, albeit at higher frequency in one of the potential sources (see
113 **Methods**).

114 To compute a signature score for a given SNV, two hypotheses are compared for each
115 potential source: (1) that one source solely explains the observed allele counts in the sink and (2)
116 all sources except that one source collectively explain the observed allele counts in the sink. For
117 each hypothesis, we calculate the binomial log-likelihood for the estimate of the allele frequency
118 in the sink, θ .

119 **Hypothesis 1:** Source i with allele frequency p_i explains the allele counts in the sink.

$$\hat{\theta} = p_i$$

120 **Hypothesis 2:** A combination of all other sources except i (sources $j \neq i$) explain the observed
121 allele count distribution in the sink. The estimate of the sink allele frequency is computed using a
122 mixture of the allele frequencies p_j from those sources. The mixing parameter α_j is learned using
123 Sequential Least Squares Programming with the constraint that $\sum_{j \neq i} \alpha_j = 1$.

124

125 The binomial log-likelihood is calculated as follows, where there are n reads with the reference
126 allele and m reads with the alternative allele in the sink.

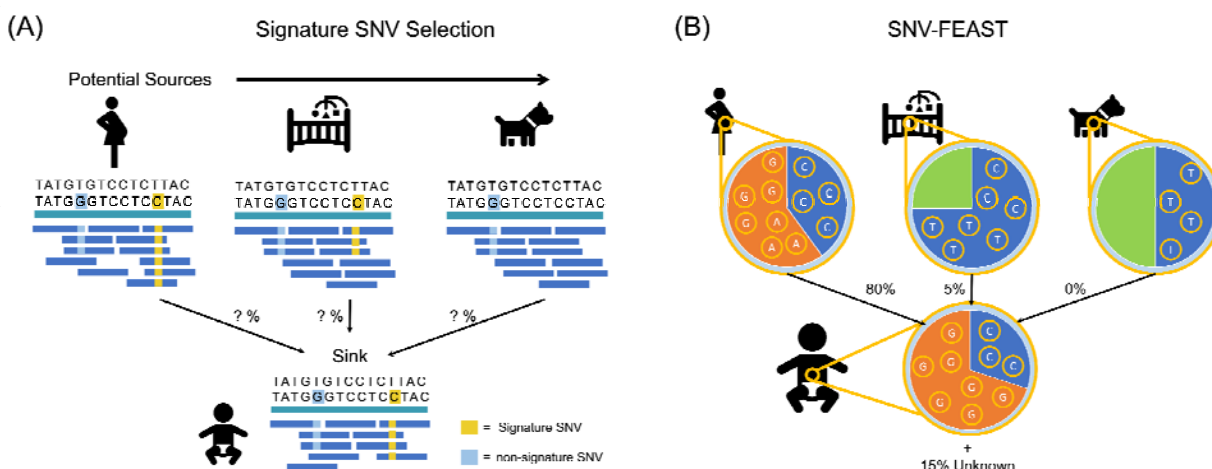
127

128

129 A log likelihood ratio representing the support for hypothesis 1 relative to hypothesis 2 is
130 calculated per site per potential source. The maximum log likelihood ratio per site is the
131 signature score for that SNV, representing how favorably one of the sources explains the sink
132 over all other sources. Signature SNVs are those with scores greater than two standard deviations
133 over the mean signature score computed for all SNVs (Methods).

134

135



136

137 **Figure 1:** Signature SNV selection and SNV-FEAST. (A) A signature SNV is present in one or
138 few but not all sources. By contrast, a non-signature SNV is generically present in multiple
139 sources and thus provides little discriminating information. (B) SNV-FEAST estimates the
140 proportion a given sink derived from various sources using the read counts for each allele in
141 sinks and sources.

142

143

144 **Evaluation of SNV-FEAST in simulations**

145 To compare the accuracy of species-FEAST and SNV-FEAST, we performed simulations
146 mimicking mother-infant transmissions with the goal of estimating contributions of different
147 sources to an infant sink. Our simulations tested the ability of SNVs and species to recapitulate
148 the true source composition in synthetic samples comprised of a mixture of reads drawn from
149 multiple real fecal adult samples. To construct these synthetic infant microbiomes, we mixed
150 metagenomic data from mothers sampled in a mother-infant dataset (Bäckhed et al., 2015) at
151 various proportions as described below (**Methods**).

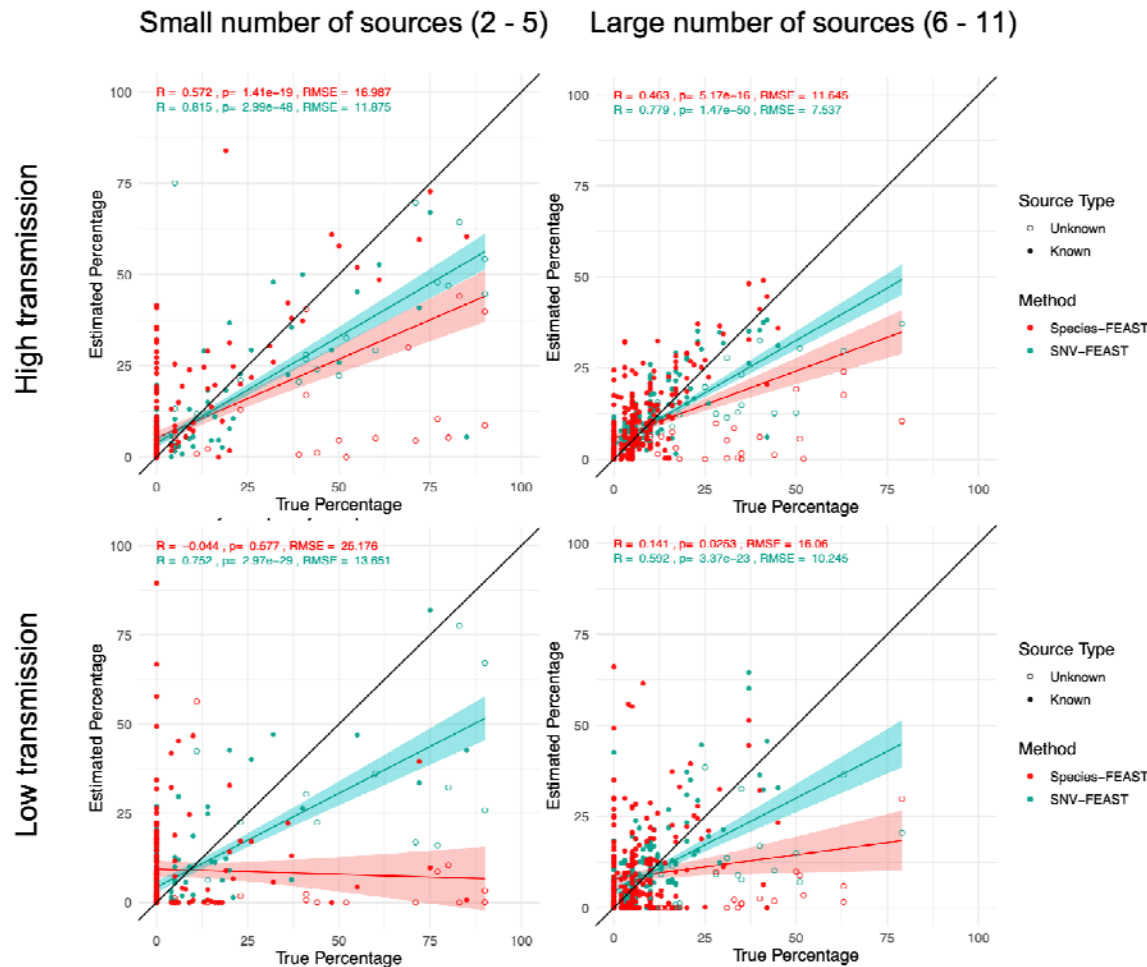
152 The difficulty of source tracking increases with the number of contributing sources
153 (Shenhav et al., 2019). Thus, we simulate infants that have a small (≤ 5) versus large (6 – 10)
154 number of contributing sources (**Supplementary Table 1**), including an unknown source (e.g. a
155 randomly selected unrelated mother). Known source contributions to the simulated gut
156 microbiome sample of the infant were varied between 1 and 90% while the unknown
157 contribution varied between 10 and 90%. The unknown source was not presented to FEAST as a
158 potential known source.

159 Additionally, not all species in a mother are transmitted to the infant (Asnicar et al.,
160 2017b; Ferretti et al., 2018; Korpela et al., 2018; Sprockett et al., 2020; Yassour et al., 2018).
161 Thus, in our simulations, species transmission rates were determined using a beta distribution,
162 which is a natural model for values between (0,1) and often proposed for microbial abundance
163 data (E. Z. Chen & Li, 2016; Martin et al., 2020; Sloan et al., 2006, 2007) (see **Methods**). We
164 therefore consider four simulated scenarios: a combination of low versus high number of sources
165 and low versus high transmission rates (see **Methods**).

166 **Figure 2** compares the performance of SNV-FEAST and species-FEAST in estimating
167 the true contribution of sources. FEAST using SNVs has equal if not better performance than
168 species in most scenarios, and performs especially well when transmission rates are low and
169 unknown source proportions are high. SNVs have a lower root mean squared error (RMSE)
170 compared to species in three of the four scenarios and higher Pearson correlation between true
171 and estimated contributions in all four scenarios. The difference in these correlations for SNVs
172 versus species is significant in all four cases when using a paired Wilcoxon signed rank test (high
173 transmission: p-value = 0.00560, 0.00251 for small and large number of sources, low
174 transmission: p-value = 0.00024, 0.002340 for small and large number of sources). These results
175 suggest that SNVs may offer useful signatures of transmission.

176

177



178

179 **Figure 2: Ability of SNV and species-FEAST to recapitulate true contributions in**
180 **simulations.** Estimated known and unknown source proportions for infant microbiomes
181 simulated with in silico mixtures of real maternal fecal microbiomes under different scenarios:
182 either low number of contributing sources (<=5) or high number of sources (6-11), and high
183 transmission rate of species or low transmission rate. Transmission rate is the probability of an
184 infant being colonized by a given species, simulated using a beta distribution centered on the
185 relative abundance of species in sources (**Methods**). 23 infants were simulated with five or fewer
186 sources and 19 infants were simulated with a large number of sources (**Table S1**). The black line
187 indicates the ground truth for proportions. For each simulated infant, there are 11 points plotted,

188 whereby 10 correspond to known sources (some of which have zero contribution), and one
189 corresponds to an unknown source which are indicated by a hollow circles in the plot.

190

191 To assess whether all species and all signatures SNVs in the sink are needed for accurate
192 source tracking, we varied the proportion of species (from 10%, 50% or 100%) and SNVs (from
193 10%, 50% or 100%) included as inputs to the algorithm (**Figure S1**). We used Pearson
194 correlation between the true and estimated proportions to represent accuracy of SNV-FEAST.
195 When decreasing the percentage of SNVs used, there is no statistically significant change in the
196 performance. However, when decreasing the percentage of species used, there are statistically
197 significant decreases in the performance (**Figure S1**).

198 To illustrate the advantage of SNV-FEAST over traditional strain tracking approaches
199 such as inStrain (Olm et al., 2021), we used the same synthetic communities produced in the
200 above simulation for inStrain profiling between each infant and each of their potential
201 contributing sources (**Figure S2**). InStrain computes a popANI score, which represents the
202 average nucleotide identity between two different metagenomic samples for a given species. As
203 per the inStrain paper, popANI values $> 99.999\%$ represent the same strain for that species being
204 shared between samples (**Methods**). However, this approach provides a binarization as to
205 whether or not a strain was transmitted, and does not account for the relative abundance of the
206 strain in the sink. Thus, we computed the fraction of each infant's species that have popANI
207 $\geq 99.999\%$, with each potential source.

208 As expected, both SNV-FEAST and inStrain produce estimates of sharing that correlate
209 positively with the ground truth mixture proportions of the contributing source samples in each
210 infant (**Figure S2**). We found inStrain results yielded a 0.742 Pearson correlation ($p < 1 \times 10^{-12}$)
211 with the true mixture proportions, whereas SNV-FEAST has a 0.866 Pearson correlation ($p < 1 \times$
212 10^{-12}) with the true proportions. The higher correlation values for SNV-FEAST likely reflect that
213 relative abundances of strains and their genomic identities are simultaneously taken into account
214 for source tracking, whereas inStrain only accounts for genomic identities. Finally, several of the
215 shared species in the simulations had popANI values $< 99.999\%$, reflecting the complex
216 mixtures from multiple sources.

217 We next compared SNV-FEAST with the strain tracking procedure in Nayfach et al.
218 2016. Again, we used the same synthetic communities produced in the simulation to determine

marker alleles as defined in Nayfach et al. 2016 (**Methods**). Here a marker allele is determined to be a SNV that is private to mother, infant, or the mother-infant dyad, and absent from the background population, which consisted of other samples in the dataset as well as samples from United States adults in the Human Microbiome Project (**Methods**). Species with $\geq 5\%$ marker allele sharing between mother and infant were deemed to share a strain (**Methods**). We found a high correlation between the true mixture proportions (on x-axis) and the percentage of species with transmission events (y-axis) (Pearson correlation 0.915, $p < 1 \times 10^{-16}$). The higher correlation for the Nayfach et al. 2016 approach compared to the inStrain approach possibly reflects horizontal gene transfers between lineages residing in infants and mothers. By contrast, there was a lower correlation between the true mixture proportions (x-axis) and the sharing for all marker alleles across species present in the infant (y-axis) and (0.575 Pearson correlation, $p < 1 \times 10^{-16}$) (**Figure S3B**).

231

232 **Source tracking in infants over the first year of life**

Having assessed the abilities of SNV-FEAST in synthetic data, we next estimated the contribution from the true mother over time to the true infant with SNV and species-FEAST in the Backhed et al. 2015 dataset. This dataset is composed of metagenomic samples from infants collected at four days, four months, and 12 months after birth, as well as their mothers at the time of delivery. Previous analyses on this data have shown that even while species similarity increases, infants and their mothers share fewer proportions of strains over time as revealed by sharing of SNVs private to mother-infant dyads (Nayfach et al., 2016). Thus, SNVs belonging to strains shared only by the infant and their mother may be more informative of the true source compared to species. Here we sought to test whether SNV and species-FEAST recapitulate these results (**Methods**).

In applying FEAST to the Backhed et al. 2015 dataset, we estimated the proportion of infant at birth attributable to mother. For 4 month infants, we estimated the proportion attributable to the mother and itself at birth. For 12 month infants, we estimated the proportion attributable to the mother and itself at birth and four months (Shenhav et al. 2019). This allowed “unknown” to be more strictly defined as the component of the infant microbiome that could not be explained by the mother. It also allowed us to better discern if completely new strains were

249 acquired at the 4th and 12th months of life (that were not already acquired during previous life
250 stages).

251 First, consistent with previous findings made with species and SNVs (Nayfach et al.,
252 2016), species-FEAST estimates an increasing contribution of the mother over time (t-test p-
253 value = 5.1×10^{-4}), but SNV-FEAST estimates a decrease over time (p-value = 0.063) (**Figure**
254 **3**).

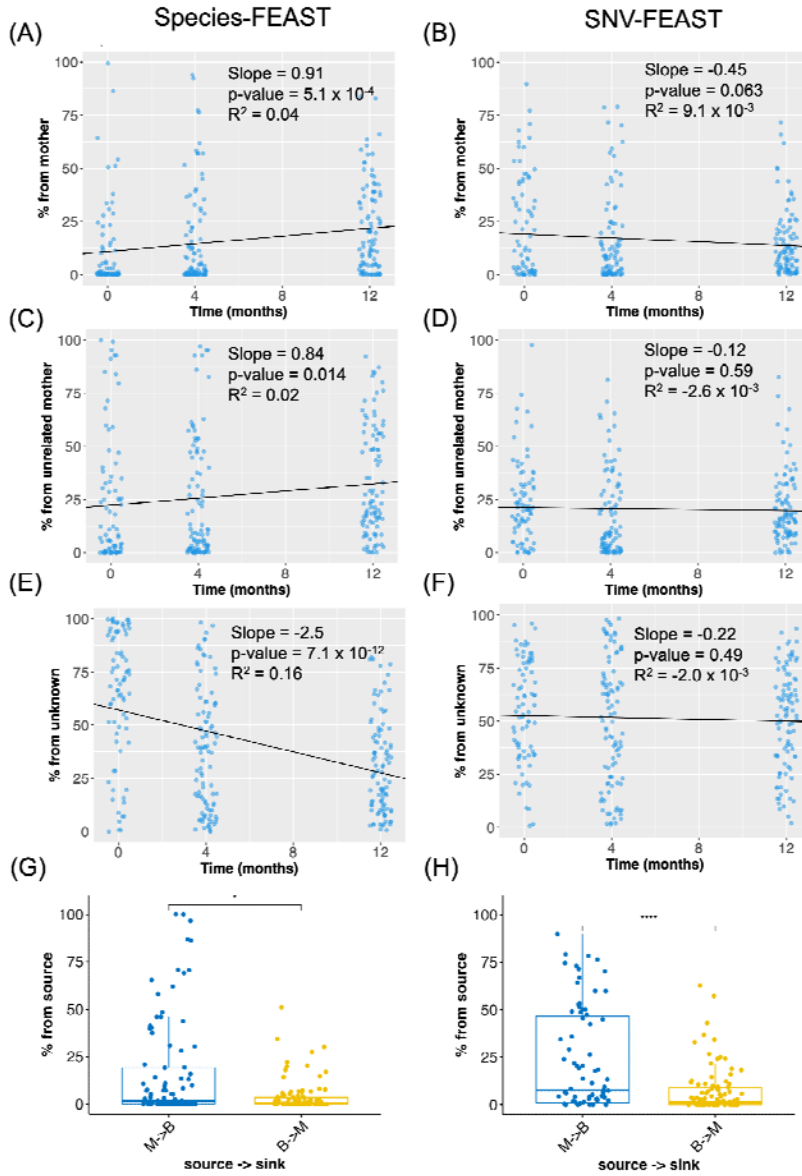
255 Second, we assessed the ability of species and SNV-FEAST to distinguish the true
256 mother from three randomly selected unrelated mothers. Species-FEAST estimates an increasing
257 contribution of unrelated mothers over time (t-test p-value = 0.014) while SNV-FEAST
258 estimates no significant change over time (t-test p-value = 0.59) (**Figure 3**). The increase in
259 contribution from unrelated mothers with species-FEAST does not suggest that these particular
260 unrelated mothers are seeding the infant. Rather, the opposing trend observed with SNVs
261 suggests that similarity at the species level is consistent with the maturation of the infant
262 microbiome over time.

263 Finally, we estimated contributions from unknown sources, i.e. the proportion of the
264 infant microbiome not explainable by the true mother, the three randomly selected unrelated
265 mothers, or any previous time point. Species-FEAST estimates a sharp decline in contribution of
266 unknown sources over the first year of life (t-test p-value = 7.1×10^{-12}) (**Figure 3**). This
267 significant decrease in unknown at the species level reflects the infant microbiome maturation
268 over the first year of life. By contrast, SNV-FEAST estimates little change in the contribution of
269 unknown sources (t-test p-value = 0.49) (**Figure 3**). Note that this unknown component reflects
270 what was gained since a previous time point. In other words, at 12 months, the infant on average
271 acquired the same fraction of unknown as it did at 4 months and birth. When source tracking is
272 run without including previous time points as sources, the unknown component increases over
273 the first year of life for SNVs only (**Figure S5**).

274 Next, we sought to understand the effect of swapping sink and source in the re-analysis of
275 Backhed et al. 2015 data. In **Figure 3G and H**, the infant at birth is the potential source and
276 mother is the sink. The estimated contribution from baby to mother is significantly smaller
277 (species-FEAST: 11.9 difference, Wilcoxon rank sum test p-value = 0.013; SNV-FEAST: 16.0
278 difference, p-value = 2.2×10^{-5}) compared to that of mother to baby. This trend may be

279 suggestive, but is not conclusive, of directionality, whereby a less diverse source is seeded by a
280 more diverse source.

281



282

283 **Figure 3. Source tracking in the infant gut microbiome over the first year of life.** Species-
284 and SNV-FEAST were applied to Backhed et al. 2019 data to estimate the contribution of (A, B)
285 mother, (C, D) unrelated mothers and (E, F) unknown sources to infants sampled at birth, four
286 months, and twelve months. The black line and inset statistics pertain to the linear regression fit
287 for the source estimates as a function of age of the infant. (G, H) are flipped source tracking
288 analyses with mother and infant swapped when using species-FEAST and SNV-FEAST,

289 respectively. **Figure S4** shows the species that were included in species-FEAST and species that
290 had SNVs included in SNV-FEAST. **Figure S5** shows the estimate of the unknown component
291 when previous time points of the infant are excluded from the sources.

292

293 **Contribution of the NICU built environment to infant microbiomes**

294 Next, we re-analyzed a metagenomic dataset studying the contribution of the hospital
295 environment to the infant gut microbiome in the neonatal intensive care unit (NICU) (Brooks et
296 al. 2017). This dataset is composed of microbiomes of infant stool, as well as the NICU rooms of
297 the same infants at frequently touched surfaces, sink basins, the floor, and isolette-top sampled
298 over an 11-month period (Brooks et al., 2017). We applied SNV and species-FEAST to assess
299 the contribution of the infant's own NICU room as well as a different NICU room in the vicinity
300 of the infant's gut microbiome (see **Methods**).

301 Concordant with the findings of Brooks et al., both SNV and species-FEAST detected
302 that the most common source contributing to the infant microbiome was the floor and isolette-top
303 from the infant's own room (**Figures 4A and B**). SNV-FEAST found Infant 18 also had large
304 contributions from their own room's touched surfaces at multiple time points (**Figure 4B**), which
305 is consistent with a finding by Brooks et al. that three strains found in Infant 18 perfectly
306 matched (> 99.999% average nucleotide identity) strains found in the touched surfaces samples
307 of Infant 18's own room. Lastly, both species-FEAST and SNV-FEAST found Infant 6's
308 microbiome was explained almost entirely by samples from a different room with SNV-FEAST
309 finding a sizeable contribution from both the floor and isolette top and the sink basin in this
310 different room. This is concordant with Brooks et al.'s finding of multiple cases of strain sharing
311 across rooms of Infant 6 and 12 for the different surfaces. FEAST with both data types is able to
312 quantify the extent to which Infant 6's microbiome was influenced by strains present in the built
313 environment.

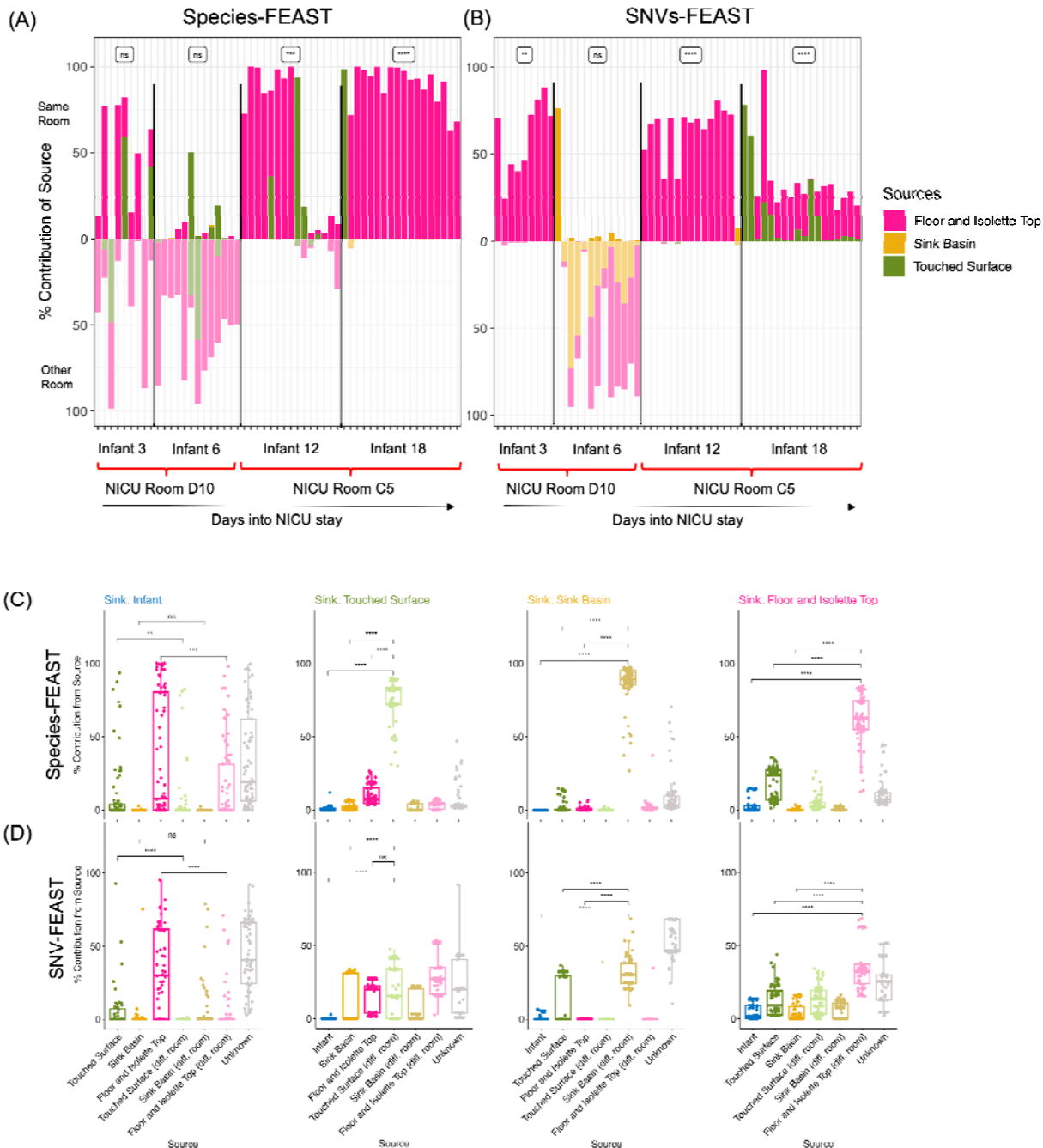
314 Through application of SNV and species-FEAST, we are able to quantify any trends over
315 time the influence of the built environment on the infant microbiome (**Figures 4A and B**). SNV-
316 FEAST more consistently finds that contribution from the infant's own room exceeds
317 contributions from a different room over time (paired Wilcoxon signed rank test for same room >
318 different room: Infant 3: p-value = 1.95×10^{-9} , Infant 6: 1, Infant 12: 3.05×10^{-5} , Infant 18: 3.81×10^{-6}) as compared to species-FEAST (Infant 3: p-value = 0.41, Infant 6: 1, Infant 12: 5.8×10^{-4} ,

320 Infant 18: 3.81×10^6). Interestingly, species-FEAST assigns one dominant source primarily,
321 whereas SNV-FEAST more often finds a combination of sources for a given sample.

322 Additionally, both SNV and species-FEAST estimated a large unknown component for
323 all four infants, with Infant 18 showing the largest mean unknown component across the NICU
324 stay based on SNVs (**Figure S6**). This unknown component is important because it signifies the
325 extent to which other sources such as the mother and diet impact infant gut colonization.

326 We then asked the question: is the infant more explained by the built environment rather
327 than vice-versa, the built environment is more explained by the infant. We tested this by
328 swapping the infant and each of the three built environment sources (**Figure 4C and D**). The
329 estimated contribution of room to infant is significantly higher than the estimated contribution of
330 infant to room, but this asymmetry is more pronounced with SNV-FEAST. SNV-FEAST showed
331 significantly higher contribution of room to infant for two of the three surface types (floor and
332 isolette top: Wilcoxon rank sum test p-value = 7.00×10^{-9} , touched surface: p-value = 0.0058,
333 sink basin: p-value = 0.274) while species-FEAST found this to be true for one of the three
334 surface types (floor and isolette top: Wilcoxon rank sum test p-value = 7.1×10^{-5} , touched
335 surface: p-value = 0.968, sink basin: p-value = 0.998). Interestingly, the built environments of
336 different rooms highly resemble each other. This is especially apparent with species-FEAST,
337 suggestive of similar ecological forces operating in similar built environments. By contrast,
338 SNV-FEAST reveals a higher diversity of contributing sources of the built environment samples
339 to other NICU built environments, once again highlighting the utility of performing source
340 tracking with SNVs.

341



349 and isolette top surface. The asterisks represent the result of a paired Wilcoxon signed rank test
350 indicating whether the total contribution of surfaces from the infant's own room were higher than
351 contributions from the other room: **** for p-value < 0.0001, *** for p-value < 0.001, ** for p-
352 value < 0.001, * for p-value < 0.05, and n.s. for p-value > 0.05. Iterative swapping of the infant
353 sink and each potential source for source tracking with (C) species-FEAST and (D) SNV-
354 FEAST. The first column shows source tracking results in which the infant was treated as the
355 sink. In each column after the first column, a different environmental source was swapped with
356 the infant and considered as a sink.

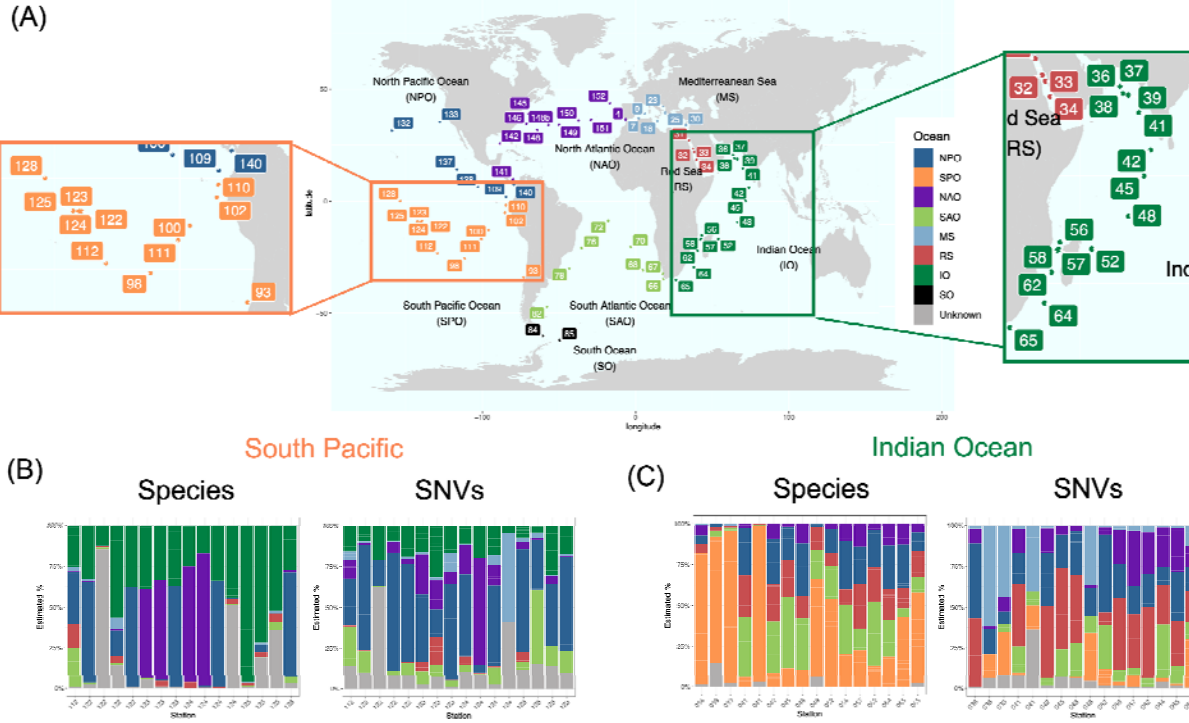
357

358 **Global source tracking of ocean microbiomes**

359 The ocean microbiome is a complex community that displays biogeography at the species
360 and functional levels (Nayfach et al., 2016; Sunagawa et al., 2015). To further understand global
361 patterns of ocean microbiomes, we applied SNV and species-FEAST to the Tara Oceans
362 microbiome dataset (Sunagawa et al., 2015). In the source tracking context, rather than defining
363 sharing as evidence of a transmission event (which is more likely in mother-infant data),
364 estimated source contributions at best explain the extent to which a given ocean sample
365 resembles other ocean samples. On one extreme, an ocean sample might be entirely explainable
366 by a single ocean's samples, and at the other extreme, an ocean sample might be explainable by
367 multiple oceans at the same time. Another alternative is for an ocean sample to not be
368 explainable by any of the provided sources, resulting in a high unknown component and
369 potentially suggesting high endemism. These source tracking estimates could be indicative of the
370 extent to which oceans mix or may be reflective of similar niches.

371 Tara Oceans is composed of 182 whole metagenomic sequencing samples derived from
372 64 stations at multiple depths. Previous research indicates that temperature is one of the highest
373 drivers of variability in microbial composition in the ocean (Ladau et al., 2013; Sunagawa et al.,
374 2015). For this reason, we restricted the source tracking analysis to sinks and sources from the
375 same temperature and depth range: above 20 degrees Celsius and within an average of 5 meters
376 below the surface.

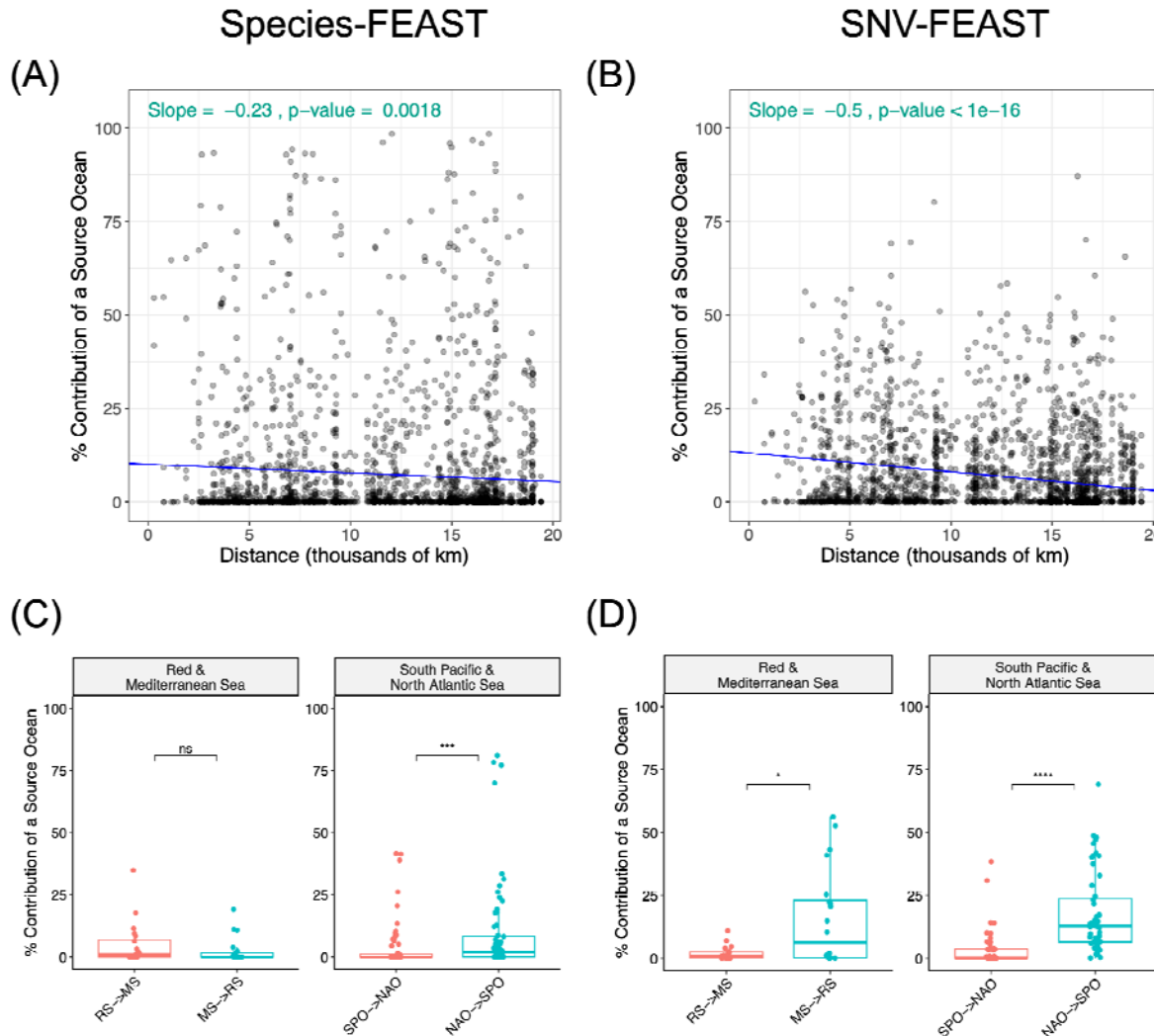
377



378

379 **Figure 5. Microbial source tracking in the Tara Oceans dataset with SNV and species-**
380 **FEAST.** World map indicating the location of sampling sites (A). Source tracking estimates for
381 the contribution of different oceans to the South Pacific (n=16) (B) and Indian Oceans (n=16)
382 (C) are depicted with vertical bars. In each experiment, all stations around the world excluding
383 those from the “sink” ocean are considered potential sources. Light blue, for example, represents
384 the total contribution of the four stations from the Mediterranean Sea that had samples in the
385 surface layer that were also greater than 20°C in temperature.

386



387

388 **Figure 6. Source tracking with ocean samples.** Distance decay in contribution of a “source”
389 ocean to a “sink” ocean when using (A) species-FEAST and (B) SNV-FEAST. In each
390 experiment, only stations from one ocean were considered as sources for a given sink station. For
391 example, when performing source tracking between the mediterranean and north atlantic, for
392 each mediterranean station, the 10 available north atlantic stations were considered as potential
393 sources. Thus, plotted are 10 points for a given mediterranean sink, where each point represents
394 the contribution of a source station from the North Atlantic to the Mediterranean sink station in
395 question. Shown in inset text are the slope and t-test p-value for the slope. (C) and (D) are
396 flipped source tracking analysis with the Red Sea and Mediterranean, as well as the South Pacific
397 Ocean and North Atlantic Ocean using species-FEAST and SNV-FEAST, respectively.

398

399 First, we performed source tracking between oceans using SNV and species-FEAST. We
400 treated each station around the world as a sink and estimated the contribution of different oceans
401 around the world to that sink (**Methods**). Unknown represents any portion of the microbiome in
402 these sink samples that cannot be explained by any of the provided source samples. We found
403 that species and SNV-FEAST estimate different amounts of sharing between oceans, where
404 SNVs estimate a higher unknown on average, potentially indicative of endemism. The finding
405 that SNV-FEAST estimates a higher unknown contribution on average is most evident in the
406 North Pacific, North Atlantic, South Atlantic, and Mediterranean oceans (**Figure S7**).
407 Additionally, in some oceans, SNVs identify contributions from oceans that species-FEAST does
408 not detect (**Figure 5, Figure S7**). For example, in applying FEAST to Indian Ocean samples we
409 find that there is measurable sharing of microbes with the Mediterranean Sea, but this is not
410 detected with species (**Figure 5C**). Such differences were found in samples from other oceans as
411 well (**Figure S7**).

412 Next, we assessed whether source tracking estimates display a distance-decay
413 relationship. Previous studies found that genetic distance, such as that represented by fixation
414 index F_{ST} , increases with geographic distance between populations (Cavalli-Sforza & Feldman,
415 2003; DeGiorgio & Rosenberg, 2013). Based on these findings, our expectation was that samples
416 that are further away from a given station will have reduced resemblance to that station. To
417 assess this distance-decay relationship, we plotted pairwise source tracking results across all
418 possible pairs of ocean samples (**Figure 6A and B**). We found that indeed as the distance
419 increases, the % explainability of a given source ocean decreases -0.23 % per thousand km
420 according to species-FEAST (t -test p -value $< 1 \times 10^{-16}$), and -0.5% per thousand km according to
421 SNV-FEAST (t -test p -value = 0.0018). The steeper slope for SNV-FEAST suggests that SNVs
422 may be more sensitive to distance decay signals on a global level.

423 Finally, we investigated whether some oceans have higher estimated contributions to
424 other oceans than vice versa, potentially indicative of the directionality of transmissions (though
425 see Discussion). Specifically, we investigated the relationship between the Red Sea to the
426 Mediterranean Sea (**Figure 6C and D**). Migration from the Red Sea to the Mediterranean,
427 known as Lessepsian migration, is well-documented for not only microorganisms but also
428 macroorganisms like fish (Bentur et al., 2008; Bianchi & Morri, 2003; Golani, 2009). Anti-
429 Lessepsian migration (Red Sea to Mediterranean), on the other hand, has been primarily thought

430 to be rare due to the Additionally, recent studies suggest that there is also evidence for anti-
431 Lessepsian migration of bacteria (Mediterranean to Red Sea) may be more common than
432 Lessepsian migration (Elsaeed et al., 2021). Research studies find that Mediterranean has brine
433 pools that produce similar a similar environment to the Red Sea's (Antunes et al., 2011),
434 allowing for bacteria from the MS to potentially thrive in the RS.

435 By swapping the Red Sea and Mediterranean as source and sink, we found that there was
436 indeed a significant difference in the estimated contribution from one direction to another with
437 SNVs but not species (**Figure 6C and D**). SNV-FEAST found the Mediterranean explained an
438 average of 15% of the Red Sea, while the Red Sea explained an average of 1.8% of the
439 Mediterranean (Wilcoxon rank sum test, p-value =0.02), consistent with anti-Lessepsian
440 migration. Meanwhile, a similar analysis with species-FEAST found the Mediterranean
441 explained 2.5% of the Red Sea and the Red Sea explained 4.9% of the Mediterranean (Wilcoxon
442 rank sum test, p-value = 0.25). In a similar analysis between North Atlantic and South Pacific we
443 found that both species and SNVs supported significantly greater contributions from the North
444 Atlantic to the South Pacific, with SNV-FEAST estimating a greater contribution (17%,
445 Wilcoxon rank sum test p-value = 5.1×10^{-11}) than species-FEAST (10%, Wilcoxon rank sum
446 test p-value = 1.8×10^{-4}).

447 Together, these results suggest that on average, SNV and species FEAST generate similar
448 source tracking results in the Tara Oceans dataset, with SNVs displaying stronger signals of
449 endemism, distance-decay relationships, and potential directionality of transmission.

450
451

452 DISCUSSION

453 Source tracking provides insight into potential source contributions to a metagenomic
454 sample as well as similarities between metagenomic samples. While species abundances have
455 been informative in source tracking in several studies (Flores et al., 2011; Knights et al., 2011;
456 McGhee et al., 2020; Shenhav et al., 2019), they may be limited in their resolution. SNVs
457 provide a potential alternative because of their ability to distinguish sources of strain
458 transmissions. Here we compared the ability of a previously published source tracking algorithm
459 FEAST using species versus SNVs as input data. In application of species and SNV-FEAST to
460 simulations as well as three case studies, we demonstrate that the two input types can provide

461 distinct insights into microbial sharing and similarities across different environments. As a
462 hypothetical example, two unrelated samples may have very similar species composition due to
463 similar colonization processes and similar environmental influences without any actual microbial
464 sharing. It would be unlikely for these two unrelated samples to share rare SNVs, however. This
465 distinction suggests that SNVs indeed can provide insight into the ecological processes shaping
466 microbial communities that species information alone cannot, and our three case studies are able
467 to demonstrate this.

468 In the first case study, we confirmed previous findings that SNV sharing between
469 mothers and infants decreases over the first year of life while species sharing increases (Nayfach
470 et al., 2016), suggesting that while the infant microbiome matures to resemble adults at the
471 species level, sources other than the mother may seed the infant over time. In the second case
472 study, we confirmed source contributions from the NICU built environment to the infant
473 microbiome (Brooks et al., 2017), and found that SNVs detect a more consistent estimate in
474 source contributions overtime compared to species as well as detecting contribution from sources
475 not detectable by species-FEAST.

476 In the third case study, we perform source tracking in the Tara oceans dataset and found
477 SNVs display a stronger distance decay relationship. These distance-decay results parallel recent
478 findings made with gene content (Dlugosch et al., 2022). While previous studies have examined
479 the biogeography of the ocean using species profiles, genes (Dlugosch et al., 2022; Nayfach et
480 al., 2016) or amino acid variants from a single species (SAR11) (Delmont et al., 2019), for the
481 first time, we leverage the use of SNVs across all detected prevalent species in the ocean
482 microbiome to identify proportions of sharing across oceans. A benefit of using SNVs in the
483 ocean microbiome is that SNVs can track fragments of DNA that have moved due to horizontal
484 gene transfer in the distant past rather than relying on inference of whole genomes or presence of
485 private SNVs that may have been transmitted in the recent past. This global-level source tracking is
486 analogous to admixture estimation with human genotypes (Alexander et al., 2009; Chiu et al.,
487 2022).

488 We note that source tracking provides insights into similarities between microbiomes and
489 potential transmissions, though the directionality is less conclusive. It is possible that increased
490 contributions in one direction but not the other is suggestive of directionality of transmission. For
491 example, in the case of the mother-infant data from Backhed et al. 2015, FEAST predicted

492 higher contribution from mother to baby than vice versa. This is consistent with work done on
493 crAss-like phage transmissions between mother and infant in the same dataset that showed
494 evidence of directionality by tracking the accumulation of mutations over time that are private to
495 the infant and absent from the mother (Siranosian et al., 2020). But in the case of the ocean, it is
496 possible that over longer time periods, differences in relative contributions from one part of the
497 world to another (e.g. Mediterranean to Red Sea) are more reflective of local selection pressures
498 that permit certain species and genotypes (Delmont et al., 2019). Thus, source tracking in certain
499 instances, such as the ocean microbiome, at best reflects the extent of similarity between samples
500 and is less conclusive about directionality.

501 A popular approach used to track strain transmissions is by detecting high average
502 nucleotide identity (ANI) for species shared between source and sink. For example, inStrain
503 (Olm et al., 2021) identifies a match between samples for a given species when ANI exceeds
504 99.999%. However, it is to be noted that inStrain provides distinct and complementary
505 information from FEAST given its binarization of whether or not a strain is shared. For
506 illustration purposes, if an infant harbors 100 species, of which only 1 came from their mother,
507 but that species' strain's relative abundance is 50% of the infant's microbiome, SNV-FEAST
508 would infer that the mother's contribution is 50%, while inStrain would infer that only 1/100th of
509 the species are derived from the mother.

510 Other studies rely on tracking transmissions of strains with private SNVs shared only
511 between the sink and putative source (Bäckhed et al., 2015; Korpela et al., 2018; Nayfach et al.,
512 2016; Schmidt et al., 2019). The private marker allele tracking approach in Nayfach et al. 2016
513 provides an improved estimate of true percentage of species that share some portion of their
514 genome with putative sources compared to inStrain (**Figure S2, S3**). It is possible that requiring
515 only 5% of marker alleles to be shared rather than a 99.999% ANI permits detection of
516 horizontal gene transfers between lineages residing in mothers and infants (D. W. Chen &
517 Garud, 2022; Vatanen et al., 2022). However, in FEAST, by using any SNV with an informative
518 distribution across sources as determined by our signature scoring method, we are able to
519 quantify the relative contribution of all the sampled environments and assign a proportion to
520 these putative sources. Another advantage to FEAST is that the contribution of unknown sources
521 can be quantified. For example, the significant fraction of marine biodiversity estimated to be

522 ‘unknown’ may be endemic, as previously noted in the Mediterranean (Katsanevakis et al.,
523 2014).

524 A drawback, however, with using SNVs over species is deeper, whole genome
525 sequencing is required to accurately call SNVs. Moreover, even when there is sufficient
526 coverage, there is still the challenge of a large number of SNVs. We demonstrate one way to
527 subset SNVs that uses a scoring method for informativeness, but there may yet be other methods
528 for filtering SNVs to the most informative set. Another potential caveat of SNV filtering is that
529 not all species present will be represented in the final signature SNV set (**Figure S4**). Species
530 with higher abundance are more likely to be represented in the signature SNV set. However, we
531 show that not all species need to contribute signature SNVs in order to make accurate inferences,
532 and likewise, not all SNVs are needed to make accurate inferences (**Figure S1**).

533 Ascertainment of SNVs from metagenomic data in a high-throughput manner, especially
534 common SNVs with microbiome genotyping technology (Shi et al., 2021), is becoming an
535 increasing priority for the field as metagenomic datasets become more abundant. A genotyper for
536 prokaryotes has already been developed and tested on a catalog of over 100 million SNVs in
537 order to characterize population structure (Shi et al., 2021). Such a catalog of informative SNVs
538 could be invaluable for source tracking. With source tracking enabling us to characterize samples
539 by their relationship to known samples, we have a powerful tool to explore samples in new
540 contexts we have yet to discover.

541

542 METHODS

543 *Data*

544 For simulations and analyses of infant microbiomes in the first year of life (Bäckhed et
545 al., 2015), we downloaded the raw shotgun metagenomic sequencing reads from public read
546 archives under accession number PRJEB6456. We downloaded the raw sequence reads for the
547 NICU analysis (Brooks et al., 2017) from accession number PRJEB323631, and the equivalent
548 for the Tara Oceans analyses (Sunagawa et al., 2015) were downloaded from accession number
549 PRJEB402. Data from the HMP Consortium (Methé et al., 2012) and Lloyd-Price et al (Lloyd-
550 Price et al., 2017) was downloaded from the following
551 URL: <https://aws.amazon.com/datasets/human-microbiome-project/>.

552

553 *Estimation of species and SNV content of metagenomic samples*

554 We used MIDAS (Metagenomic Intra-Species Diversity Analysis System, version 1.2,
555 downloaded on November 21, 2016 (Nayfach et al., 2016) to estimate species abundance and SNV
556 content per species in each metagenomic shotgun sequencing sample. The database we used to apply
557 MIDAS consisted of 31,007 bacterial genomes that are clustered into 5,952 species. The parameters we
558 used to estimate species abundances and SNVs were described in (Garud et al., 2019). A species was
559 considered present if there are at least 3 reads mapping to a set of single copy marker genes on average.
560 To call SNVs, we used the default MIDAS settings in order to map reads to a single representative
561 reference genome. The mapping was done with Bowtie 2 (Langmead & Salzberg, 2012): global
562 alignment, $\text{MAPID} \geq 94.0\%$, $\text{READQ} \geq 20$, $\text{ALN_COV} \geq 0.75$, and $\text{MAPQ} \geq 20$, where species with reads
563 mapped to less than 40% of the genome were excluded from the SNV calls. We excluded samples with
564 depth lower than 5 reads, and excluded genetic sites using the default site filters of MIDAS (e.g.
565 $\text{ALLELE_FREQ} \geq 0.01$, with the exception of SITE_DEPTH which was set to 3.

566

567 *Application of FEAST algorithm*

568 FEAST, originally introduced by Shenhav et al., is an R-based method that models the
569 mixture proportions for various “source” microbial samples for a given “sink” (Shenhav et al.,
570 2019). This method utilizes expectation maximization to estimate the proportions when given
571 any sort of count-based feature matrix representing the potential sources and sinks. The intuition
572 behind the estimation process is that a source with a similar species distribution to the sink would
573 have a higher contribution estimate to the sink. A species with non-zero counts only in source j
574 and the sink would increase the estimated contribution of source j . However, in many cases, the
575 same species are found in multiple sources simultaneous. The algorithm does not uniquely assign
576 a species to a source but rather simultaneously utilizes all species information to infer the source
577 contributions. The method was originally tested and evaluated on species and not on more fine
578 scale genetic data such as SNVs. The number of different species, on average, range in number
579 from a few hundred to a few thousand, while the number of possible nucleotide sites that vary
580 across different sources can number in millions. For this reason, a SNV-filtering process is
581 necessary so that the algorithm can run within a reasonable time and with reasonable memory
582 requirements.

583

584 *Application of FEAST to the Backhed et al. 2015 dataset:*

585 For both species and SNV-FEAST, the same set of sources and sinks were fed into the
586 FEAST algorithm. In the case study of infants in the first year of life (Bäckhed et al., 2015), the
587 sink consisted of the infant fecal sample at either four days, four months, or 12 months and the
588 potential sources consisted of fecal samples from the true mother, three randomly selected
589 mothers from the same dataset, and also any previous time points for the infant.

590 Species-FEAST utilized all species present in the infant whereas SNV-FEAST used
591 signature SNVs from the subset of species that had signature SNVs. Shown in **Figure S3** are the
592 distribution of species included in species and SNV-FEAST.

593

594 *Application of FEAST to the Brooks et al. 2017 dataset:*

595 For the case study of infants in the NICU (Brooks et al., 2017), the sink consisted of the
596 fecal sample of the infant at a given time point and the potential sources consisted of pooled
597 reads from the touched surfaces, the sink basin and the floor and isolette top from both the
598 infant's own room as well as a different room. The different room was Infant 12's room for
599 Infants 3 and 6, Infants 6's room for Infants 12 and 18.

600

601 *Application of FEAST to the Sunagawa et al. 2015 dataset: Determining the signature SNV set*
602 Signature SNVs were identified as described in the main text. We provide specific steps for
603 determining signature SNVs:

604 (1) Filter sites: only sites of the genome with at least the required number of reads mapping
605 to the site are considered. In the case study of infants in the first year of life (Bäckhed et
606 al., 2015) and infants in the NICU (Brooks et al., 2017), the minimum coverage
607 requirement is 10 across the sink and J sources. For the Tara Ocean (Sunagawa et al.,
608 2015) samples, the minimum coverage is five reads (Sunagawa et al., 2015).

609 Additionally, sites that are biallelic must have more than one read mapped to each allele
610 to be considered.

611 (2) Perform per site per source parameter estimates: for each potential source compute the
612 estimated allele frequency in the sink $\hat{\theta}$ under two different hypotheses:

613 **Hypothesis 1:** Source i with allele frequency p_i explains the allele counts in the sink.

$$\hat{\theta} = p_i$$

614 **Hypothesis 2:** A combination of all other sources except i (sources $j \neq i$) explain the
615 observed allele count distribution in the sink. The estimate of the sink allele frequency is
616 computed using a mixture of the allele frequencies p_j from those sources. The mixing
617 parameter α_j is learned using Sequential Least Squares Programming (scipy.optimize.minimize())
618 with the constraint of summing to 1 with bounds of 0 to 1 inclusive: $\sum_{j \neq i} \alpha_j = 1$.

619

$$\hat{\theta} = \sum_{j \neq i} \alpha_j p_j$$

620 **(3)** Compute per site per source log likelihoods: Compute the binomial log-likelihood under
621 hypotheses 1 and 2, given n reads with the reference allele and m reads with the
622 alternative allele in the sink:

623

$$l(\hat{\theta}) = n \log \hat{\theta} + m \log(1 - \hat{\theta})$$

624 **(4)** Compute per site per source log likelihood ratio:

$$l_1(\theta) - l_2(\theta)$$

625

626 **(5)** Compute per site summary signature score: The maximum log likelihood ratio per site is
627 the signature score for that SNV, representing how favorably one of the sources explains
628 the sink over all other sources

629 **(6)** Filtering of SNVs using signature score: One signature score for that SNV represents
630 how favorably one source explains the sink better than all other sources. All the scores
631 are ranked across SNVs and SNVs with scores that are greater than two standard
632 deviations over the mean signature score within each 200 kbp window of the genome are
633 retained as signature SNVs. This window size was chosen for to optimize run time and
634 memory requirements.

635

636 Note, if only one source passes minimum coverage filtering, $l_2(\theta) = 0$ resulting in a
637 very high likelihood ratio as represented by $l_1(\theta)$ for the one source. These SNVs are
638 more likely to pass the signature score filtering. One exception for SNVs that are
639 included in the signature SNV set without passing signature score filtering are SNVs with
640 an allele that is completely unique to the infant, as these represent SNVs that are

641 potentially derived from an unknown source. Signature SNVs are obtained from the SNV
642 profile of every species for which there is MIDAS output.

643

644 *Simulating mother to infant transmission*

645 The mixture proportions for 28 simulated infants is shown in **Table S1**. Four possible
646 scenarios are simulated using a combination of either low or high number of sources and low or
647 high transmission probabilities of species. High transmission of species was simulated by
648 drawing separate transmission probabilities for each species in each contributing source based on
649 a beta distribution with a mean equal to the species relative abundance and variance equal to 0.1,
650 a value selected to emulate Backhed et al.’s mean relative abundance and variance. For the low
651 transmission scenario, transmission probabilities were drawn from a beta distribution with mean
652 0.1 times the relative abundance and variance at 0.1. To determine if a species from each source
653 was transmitted to a given infant, a binomial draw was performed J times, where J = number of
654 sources, and the probability of a mother transmitting the species is p_j based on the beta-drawn
655 transmission probability. If any of the draws yields a one, that species is transmitted to the infant
656 from all sources. The same simulated data under these scenarios is used for both SNV and
657 species source tracking.

658 The source tracking estimates are compared to the true mixing proportions using
659 Spearman correlation. The significance of correlation is calculated using the stat_cor function in
660 the ‘ggpubr’ package (CRAN - Package Ggpubr, n.d.).

661

662 *Comparison to inStrain*

663 We ran inStrain (Olm et al., 2021) on the same synthetic samples as described above.
664 InStrain “profile” (Olm et al., 2021) and inStrain “compare” (Olm et al., 2021) were run for
665 every possible infant-source pair. For example, for simulated infant 1 there were 10 putative
666 sources, therefore inStrain compare was run 10 times for each putative source. InStrain reports
667 popANI calculated per scaffold for a given species. To compute a single statistic per species, we
668 computed the average popANI across scaffolds for a given species. The percent infant
669 microbiome species that had strains shared with mother was computed as the number of species
670 in which popANI was $\geq 99.999\%$ divided by the total number of species with coverage ≥ 5 .
671 PopANI was only calculated in scaffolds that had ≥ 5 coverage in both samples of the pair.

672

673 *Comparison with strain tracking approach in Nayfach et al. 2016*

674 We applied the strain tracking approach in Nayfach et al. 2016 on the same synthetic
675 communities described above. In Nayfach et al. 2016, strain transmissions are tracked by
676 identifying ‘marker alleles’ which are private to the infant, mother, or infant-mother dyad, and
677 absent from the broader population. A strain is considered to be shared if at least 5% of all
678 marker alleles for a mother-infant dyad are shared. Note that the approach for strain tracking
679 proposed in Nayfach et al. 2016 utilizes SNV information outputted by MIDAS, but is not a part
680 of MIDAS.

681 Each simulated infant had up to 10 sources that were real maternal samples from
682 Backhed et al. 2015 For each possible pair of infants and maternal sources (10 pairings per
683 infant, with 48 infants), we found the set of infant-only marker alleles, mother-only marker
684 alleles, and mother-infant dyad marker alleles. As described in Nayfach et al, 2016, only sites
685 with minimum 30 reads and only alleles that were supported by at least 10% of the total reads
686 aligned to that site were considered. The infant marker allele and mother marker allele were
687 defined as alleles that were present only in the focal sample and absent from the background
688 samples (or below 3 reads = 10% * 30 reads). For the infant, the background consisted of all
689 mothers (including mothers that were used to simulate the infant), real infant samples (excluding
690 infants of mothers used to simulate the infant), and 337 samples of adults from the United States
691 in the HMP (which includes 180 unique adults) that were obtained from the metagenomics
692 repository of HMP under project ID SRP002163 and SRP056641 (Lloyd-Price et al., 2017;
693 Methé et al., 2012). For the mother, the background consisted of all mother and infant samples in
694 addition to the HMP samples. For computing shared marker alleles, an allele must be present in
695 both the mother and infant but absent from the background, which consisted of all mothers and
696 the HMP samples.

697 To compute sharing, two quantities were considered: “total sharing”, defined as % shared
698 marker alleles/ (infant marker alleles + mother marker alleles + shared marker alleles) and
699 proportion of infant marker alleles that are shared: % shared marker alleles/ (infant marker
700 alleles + shared marker alleles). The first quantity compared to FEAST estimates was the
701 percentage of infant species in which the “total sharing” was at least 5%. The second quantity

702 compared to FEAST was the pooled proportion of infant marker alleles that are shared across all
703 species.

704

705 *Distance Decay Analysis*

706 To study the relationship between source tracking estimates and geographic distance, we
707 analyzed all oceans as either a sink or source against all other possible oceans. To compute
708 geographic distance between stations, we applied the Haversine distance to the longitude and
709 latitude of the sampling sites provided by (Sunagawa et al., 2015) using the package “geosphere”
710 (Hijmans et al., 2021). Source tracking estimates were computed as described above using either
711 SNV-FEAST or Species FEAST. The regression line for the distance decay analysis was
712 computed using a linear mixed model “contribution ~ distance + (1| sink_ocean)”.

713

714 **Ethics declarations**

715 The authors declare that they have no competing interests.

716

717 **Acknowledgements**

718 We thank Nicole Zeltser for processing the Tara Oceans data through the MIDAS pipeline. We
719 thank Richard Wolff for his advice on simulations. We thank Michael Wasney for testing the
720 associated software. We thank members of the Garud lab for their feedback on the manuscript.
721 LB was supported by the NSF Graduate Research Fellowship Program grant numbers DGE-
722 1650604 and DGE-2034835. N.R.G. received support from the Paul Allen Frontiers Group and
723 the Research Corporation for Science Advancement.

724

725 **Availability of Data and Materials**

726 All metagenomic data was obtained from public repositories. The applicable accessions numbers
727 are PRJEB6456 for Backhed et al. 2015 (mother-infant), PRJEB323631 for Brooks et al. 2017
728 (NICU), PRJEB402 for Sunagawa et al. 2015 (Tara Oceans), and SRP002163 and SRP056641
729 for HMP.

730

731 Source code for SNV-FEAST signature SNV selection as well as analyses in this paper are
732 available at GitHub (<https://github.com/garudlab/Signature-SNVs>), Zenodo (DOI

733 10.5281/zenodo.7515044), and PyPi for pip installation (<https://pypi.org/project/Signature-SNVs/0.0.1/>).

735

736

737 **References**

738 Alexander, D. H., Novembre, J., & Lange, K. (2009). Fast model-based estimation of ancestry in
739 unrelated individuals. *Genome Research*, 19(9), 1655–1664.

740 <https://doi.org/10.1101/GR.094052.109>

741 Antunes, A., Ngugi, D. K., & Stingl, U. (2011). Microbiology of the Red Sea (and other) deep-
742 sea anoxic brine lakes. *Environmental Microbiology Reports*, 3(4), 416–433.

743 <https://doi.org/10.1111/J.1758-2229.2011.00264.X>

744 Asnicar, F., Manara, S., Zolfo, M., Truong, D. T., Scholz, M., Armanini, F., Ferretti, P., Gorfer,
745 V., Pedrotti, A., Tett, A., & Segata, N. (2017a). Studying Vertical Microbiome
746 Transmission from Mothers to Infants by Strain-Level Metagenomic Profiling. *MSystems*,
747 2(1). <https://doi.org/10.1128/msystems.00164-16>

748 Asnicar, F., Manara, S., Zolfo, M., Truong, D. T., Scholz, M., Armanini, F., Ferretti, P., Gorfer,
749 V., Pedrotti, A., Tett, A., & Segata, N. (2017b). Studying Vertical Microbiome
750 Transmission from Mothers to Infants by Strain-Level Metagenomic Profiling. *MSystems*,
751 2(1). <https://doi.org/10.1128/MSYSTEMS.00164-16/ASSET/54C4C531-C6DB-421B-8C8A-10C0ECFE3BE9/ASSETS/GRAPHIC/SYS0011720800004.JPG>

752 Bäckhed, F., Roswall, J., Peng, Y., Feng, Q., Jia, H., Kovatcheva-Datchary, P., Li, Y., Xia, Y.,
753 Xie, H., Zhong, H., Khan, M. T., Zhang, J., Li, J., Xiao, L., Al-Aama, J., Zhang, D., Lee, Y.,
754 S., Kotowska, D., Colding, C., ... Jun, W. (2015). Dynamics and stabilization of the human
755 gut microbiome during the first year of life. *Cell Host and Microbe*, 17(5), 690–703.
756 <https://doi.org/10.1016/j.chom.2015.04.004>

757 Bentur, Y., Ashkar, J., Lurie, Y., Levy, Y., Azzam, Z. S., Litmanovich, M., Golik, M., Gurevych,
758 B., Golani, D., & Eisenman, A. (2008). Lessepsian migration and tetrodotoxin poisoning
759 due to *Lagocephalus sceleratus* in the eastern Mediterranean. *Toxicon*, 52(8), 964–968.
760 <https://doi.org/10.1016/J.TOXICON.2008.10.001>

761 Bianchi, C. N., & Morri, C. (2003). Global sea warming and “tropicalization” of the
762 Mediterranean Sea: biogeographic and ecological aspects. *Biogeographia – The Journal of*

764 *Integrative Biogeography*, 24(1). <https://doi.org/10.21426/B6110129>

765 Brooks, B., Olm, M. R., Firek, B. A., Baker, R., Thomas, B. C., Morowitz, M. J., & Banfield, J.

766 F. (2017). Strain-resolved analysis of hospital rooms and infants reveals overlap between

767 the human and room microbiome. *Nature Communications*, 8(1), 1–7.

768 <https://doi.org/10.1038/s41467-017-02018-w>

769 Cavalli-Sforza, L. L., & Feldman, M. W. (2003). The application of molecular genetic

770 approaches to the study of human evolution. *Nature Genetics* 2003 33:3, 33(3), 266–275.

771 <https://doi.org/10.1038/ng1113>

772 Chen, D. W., & Garud, N. R. (2022). Rapid evolution and strain turnover in the infant gut

773 microbiome. *Genome Research*, 32(6), 1124–1136.

774 <https://doi.org/10.1101/GR.276306.121/-/DC1>

775 Chen, E. Z., & Li, H. (2016). A two-part mixed-effects model for analyzing longitudinal

776 microbiome compositional data. *Bioinformatics*, 32(17), 2611–2617.

777 <https://doi.org/10.1093/BIOINFORMATICS/BTW308>

778 Chiu, A. M., Molloy, E. K., Tan, Z., Talwalkar, A., & Sankararaman, S. (2022). Inferring

779 population structure in biobank-scale genomic data. *The American Journal of Human*

780 *Genetics*. <https://doi.org/10.1016/J.AJHG.2022.02.015>

781 CRAN - Package *ggbpusr*. (n.d.). Retrieved March 6, 2022, from <https://cran.r-project.org/web/packages/ggbpusr/index.html>

782 DeGiorgio, M., & Rosenberg, N. A. (2013). Geographic Sampling Scheme as a Determinant of

783 the Major Axis of Genetic Variation in Principal Components Analysis. *Molecular Biology*

784 and *Evolution*, 30(2), 480–488. <https://doi.org/10.1093/MOLBEV/MSS233>

785 Delmont, T. O., Kiefl, E., Kilinc, O., Esen, O. C., Uysal, I., Rappé, M. S., Giovannoni, S., &

786 Eren, A. M. (2019). Single-amino acid variants reveal evolutionary processes that shape the

787 biogeography of a global SAR11 subclade. *ELife*, 8. <https://doi.org/10.7554/ELIFE.46497>

788 Dlugosch, L., Poehlein, A., Wemheuer, B., Pfeiffer, B., Badewien, T. H., Daniel, R., & Simon,

789 M. (2022). Significance of gene variants for the functional biogeography of the near-surface

790 Atlantic Ocean microbiome. *Nature Communications* 2022 13:1, 13(1), 1–11.

791 <https://doi.org/10.1038/s41467-022-28128-8>

792 Elsaeed, E., Fahmy, N., Hanora, A., & Enany, S. (2021). Bacterial Taxa Migrating from the

793 Mediterranean Sea into the Red Sea Revealed a Higher Prevalence of Anti-Lessepsian

794

795 Migrations. *OMICS A Journal of Integrative Biology*, 25(1), 60–71.

796 <https://doi.org/10.1089/omi.2020.0140>

797 Ferretti, P., Pasolli, E., Tett, A., Asnicar, F., Gorfer, V., Fedi, S., Armanini, F., Truong, D. T.,
798 Manara, S., Zolfo, M., Beghini, F., Bertorelli, R., De Sanctis, V., Bariletti, I., Canto, R.,
799 Clementi, R., Cologna, M., Crifò, T., Cusumano, G., ... Segata, N. (2018). Mother-to-Infant
800 Microbial Transmission from Different Body Sites Shapes the Developing Infant Gut
801 Microbiome. *Cell Host and Microbe*, 24(1), 133-145.e5.
802 <https://doi.org/10.1016/j.chom.2018.06.005>

803 Flores, G. E., Bates, S. T., Knights, D., Lauber, C. L., Stombaugh, J., Knight, R., & Fierer, N.
804 (2011). Microbial Biogeography of Public Restroom Surfaces. *PLoS ONE*, 6(11), e28132.
805 <https://doi.org/10.1371/journal.pone.0028132>

806 Garud, N. R., Good, B. H., Hallatschek, O., & Pollard, K. S. (2019). Evolutionary dynamics of
807 bacteria in the gut microbiome within and across hosts. *PLoS Biology*, 17(1), e3000102.
808 <https://doi.org/10.1371/JOURNAL.PBIO.3000102>

809 Golani, D. (2009). Distribution of Lessepsian migrant fish in the Mediterranean.
810 <Http://Dx.Doi.Org/10.1080/11250009809386801>, 65(S1), 95–99.
811 <https://doi.org/10.1080/11250009809386801>

812 Hijmans, R. J., Karney, C., Geographiclib,] (, Williams, E., Vennes, C., & Maintainer,]. (2021).
813 *Package “geosphere.”* <https://doi.org/10.1007/s00190012>

814 Katsanevakis, S., Coll, M., Piroddi, C., Steenbeek, J., Lasram, F. B. R., Zenetos, A., & Cardoso,
815 A. C. (2014). Invading the Mediterranean Sea: Biodiversity patterns shaped by human
816 activities. *Frontiers in Marine Science*, 1(SEP), 32.
817 <https://doi.org/10.3389/FMARS.2014.00032/ABSTRACT>

818 Knights, D., Kuczynski, J., Charlson, E. S., Zaneveld, J., Mozer, M. C., Collman, R. G.,
819 Bushman, F. D., Knight, R., & Kelley, S. T. (2011). Bayesian community-wide culture-
820 independent microbial source tracking. *Nature Methods*, 8(9), 761–765.
821 <https://doi.org/10.1038/nmeth.1650>

822 Korpela, K., Costea, P., Coelho, L. P., Kandels-Lewis, S., Willemsen, G., Boomsma, D. I.,
823 Segata, N., & Bork, P. (2018). Selective maternal seeding and environment shape the
824 human gut microbiome. *Genome Research*, 28(4), 561–568.
825 <https://doi.org/10.1101/GR.233940.117/-DC1>

826 Ladau, J., Sharpton, T. J., Finucane, M. M., Jospin, G., Kembel, S. W., O'Dwyer, J., Koeppel, A.
827 F., Green, J. L., & Pollard, K. S. (2013). Global marine bacterial diversity peaks at high
828 latitudes in winter. *The ISME Journal* 2013 7:9, 7(9), 1669–1677.
829 <https://doi.org/10.1038/ismej.2013.37>

830 Langmead, B., & Salzberg, S. L. (2012). Fast gapped-read alignment with Bowtie 2. *Nature
831 Methods* 2012 9:4, 9(4), 357–359. <https://doi.org/10.1038/nmeth.1923>

832 Li, S. S., Zhu, A., Benes, V., Costea, P. I., Hercog, R., Hildebrand, F., Huerta-Cepas, J.,
833 Nieuwdorp, M., Salojärvi, J., Voigt, A. Y., Zeller, G., Sunagawa, S., De Vos, W. M., &
834 Bork, P. (2016). Durable coexistence of donor and recipient strains after fecal microbiota
835 transplantation. *Science*, 352(6285), 586–589.
836 https://doi.org/10.1126/SCIENCE.AAD8852/SUPPL_FILE/LI-SM.PDF

837 Lloyd-Price, J., Mahurkar, A., Rahnavard, G., Crabtree, J., Orvis, J., Hall, A. B., Brady, A.,
838 Creasy, H. H., McCracken, C., Giglio, M. G., McDonald, D., Franzosa, E. A., Knight, R.,
839 White, O., & Huttenhower, C. (2017). Strains, functions and dynamics in the expanded
840 Human Microbiome Project. *Nature* 2017 550:7674, 550(7674), 61–66.
841 <https://doi.org/10.1038/nature23889>

842 Martin, B. D., Witten, D., & Willis, A. D. (2020). MODELING MICROBIAL ABUNDANCES
843 AND DYSBIOSIS WITH BETA-BINOMIAL REGRESSION. *The Annals of Applied
844 Statistics*, 14(1), 94. <https://doi.org/10.1214/19-AOAS1283>

845 McGhee, J. J., Rawson, N., Bailey, B. A., Fernandez-Guerra, A., Sisk-Hackworth, L., & Kelley,
846 S. T. (2020). Meta-SourceTracker: application of Bayesian source tracking to shotgun
847 metagenomics. *PeerJ*, 8, e8783. <https://doi.org/10.7717/peerj.8783>

848 Methé, B. A., Nelson, K. E., Pop, M., Creasy, H. H., Giglio, M. G., Huttenhower, C., Gevers, D.,
849 Petrosino, J. F., Abubucker, S., Badger, J. H., Chinwalla, A. T., Earl, A. M., Fitzgerald, M.
850 G., Fulton, R. S., Hallsworth-Pepin, K., Lobos, E. A., Madupu, R., Magrini, V., Martin, J.
851 C., ... White, O. (2012). A framework for human microbiome research. *Nature* 2012
852 486:7402, 486(7402), 215–221. <https://doi.org/10.1038/nature11209>

853 Nayfach, S., Rodriguez-Mueller, B., Garud, N., & Pollard, K. S. (2016). An integrated
854 metagenomics pipeline for strain profiling reveals novel patterns of bacterial transmission
855 and biogeography. *Genome Research*, 26(11), 1612–1625.
856 <https://doi.org/10.1101/gr.201863.115>

857 Olm, M. R., Crits-Christoph, A., Bouma-Gregson, K., Firek, B. A., Morowitz, M. J., & Banfield,
858 J. F. (2021). inStrain profiles population microdiversity from metagenomic data and
859 sensitively detects shared microbial strains. *Nature Biotechnology* 2021 39:6, 39(6), 727–
860 736. <https://doi.org/10.1038/s41587-020-00797-0>

861 Schloissnig, S., Arumugam, M., Sunagawa, S., Mitreva, M., Tap, J., Zhu, A., Waller, A., Mende,
862 D. R., Kultima, J. R., Martin, J., Kota, K., Sunyaev, S. R., & Weinstock, G. M. (2013).
863 Genomic variation landscape of the human gut microbiome. *Nature*.
864 <https://doi.org/10.1038/nature11711>

865 Schmidt, T. S. B., Hayward, M. R., Coelho, L. P., Li, S. S., Costea, P. I., Voigt, A. Y., Wirbel, J.,
866 Maistrenko, O. M., Alves, R. J. C., Bergsten, E., de Beaufort, C., Sobhani, I., Heintz-
867 Buschart, A., Sunagawa, S., Zeller, G., Wilmes, P., & Bork, P. (2019). Extensive
868 transmission of microbes along the gastrointestinal tract. *ELife*, 8.
869 <https://doi.org/10.7554/ELIFE.42693>

870 Shenhav, L., Thompson, M., Joseph, T. A., Briscoe, L., Furman, O., Bogumil, D., Mizrahi, I.,
871 Pe'er, I., & Halperin, E. (2019). FEAST: fast expectation-maximization for microbial
872 source tracking. *Nature Methods*, 16(7). <https://doi.org/10.1038/s41592-019-0431-x>

873 Shi, Z. J., Dimitrov, B., Zhao, C., Nayfach, S., & Pollard, K. S. (2021). Fast and accurate
874 metagenotyping of the human gut microbiome with GT-Pro. *Nature Biotechnology* 2021
875 40:4, 507–516. <https://doi.org/10.1038/s41587-021-01102-3>

876 Siranosian, B. A., Tamburini, F. B., Sherlock, G., & Bhatt, A. S. (2020). Acquisition,
877 transmission and strain diversity of human gut-colonizing crAss-like phages. *Nature
878 Communications* 2020 11:1, 11(1), 1–11. <https://doi.org/10.1038/s41467-019-14103-3>

879 Sloan, W. T., Lunn, M., Woodcock, S., Head, I. M., Nee, S., & Curtis, T. P. (2006). Quantifying
880 the roles of immigration and chance in shaping prokaryote community structure.
881 *Environmental Microbiology*, 8(4), 732–740. [https://doi.org/10.1111/J.1462-2920.2005.00956.X](https://doi.org/10.1111/J.1462-
882 2920.2005.00956.X)

883 Sloan, W. T., Woodcock, S., Lunn, M., Head, I. M., & Curtis, T. P. (2007). Modeling taxa-
884 abundance distributions in microbial communities using environmental sequence data.
885 *Microbial Ecology*, 53(3), 443–455. [https://doi.org/10.1007/S00248-006-9141-X/FIGURES/4](https://doi.org/10.1007/S00248-006-9141-
886 X/FIGURES/4)

887 Sprockett, D. D., Martin, M., Costello, E. K., Burns, A. R., Holmes, S. P., Gurven, M. D., &

888 Relman, D. A. (2020). Microbiota assembly, structure, and dynamics among Tsimane
889 horticulturalists of the Bolivian Amazon. *Nature Communications* 2020 11:1, 11(1), 1–14.
890 <https://doi.org/10.1038/s41467-020-17541-6>

891 Sunagawa, S., Coelho, L. P., Chaffron, S., Kultima, J. R., Labadie, K., Salazar, G., Djahanschiri,
892 B., Zeller, G., Mende, D. R., Alberti, A., Cornejo-Castillo, F. M., Costea, P. I., Cruaud, C.,
893 d'Ovidio, F., Engelen, S., Ferrera, I., Gasol, J. M., Guidi, L., Hildebrand, F., ... Bork, P.
894 (2015). Structure and function of the global ocean microbiome. *Science*, 348(6237).
895 <https://doi.org/10.1126/SCIENCE.1261359>

896 Vatanen, T., Jabbar, K. S., Vlamakis, H., Knip, M., & Correspondence, R. J. X. (2022). Mobile
897 genetic elements from the maternal microbiome shape infant gut microbial assembly and
898 metabolism. *Cell*, 185, 4921-4936.e15. <https://doi.org/10.1016/j.cell.2022.11.023>

899 Yassour, M., Jason, E., Hogstrom, L. J., Arthur, T. D., Tripathi, S., Siljander, H., Selvenius, J.,
900 Oikarinen, S., Hyöty, H., Virtanen, S. M., Ilonen, J., Ferretti, P., Pasolli, E., Tett, A.,
901 Asnicar, F., Segata, N., Vlamakis, H., Lander, E. S., Huttenhower, C., ... Xavier, R. J.
902 (2018). Strain-Level Analysis of Mother-to-Child Bacterial Transmission during the First
903 Few Months of Life. *Cell Host & Microbe*, 24(1), 146-154.e4.
904 <https://doi.org/10.1016/J.CHOM.2018.06.007>

905

906